CRYSTAL GROWTH & DESIGN

Article

Cite This: Cryst. Growth Des. 2018, 18, 6497−6503

pubs.acs.org/crystal

A Novel Tautomeric Polymorph of Anhydrous Guanine and Its Reversible Water Harvesting Property

Fenghua Chen,[†] Yurong Ma,*[,‡] Yingxia Wang,[†] and Limin Qi*[,†]

[†]Beijing National Laboratory for Molecular Sciences, College of Chemistry, Peking University, Beijing, 100871, China

[‡]School of Chemistry and Chemical Engineering, Beijing Institute of Technology, Beijing, 100081, China

Supporting Information

ABSTRACT: Tautomeric isomerism is very important in DNA/RNA research, especially base-pair mismatches. However, the tautomeric polymorph of anhydrous guanine (AG) composed of a N_7-G purine ring has never been reported in the literature. Herein, a novel crystal phase of anhydrous guanine consisting of a N_9-G purine ring was obtained by dehydration of guanine monohydrate (GM) at 111 °C, termed dehydrated-GM, the first reported tautomeric polymorph of AG (N_7-G). The dehydration/hydration transformation between GM and dehydrated-GM can be repeated more than 10 times without any observable phase damage. The dehydrated-GM can harvest 8 wt % water within 30 min at relative low humidity (below 20%). Furthermore, dehydrated-GM has long-term stability in a very dry environment when the temperature is in between RT and 150 °C. The channel structure of dehydrated-GM can enlighten the design of materials to harvest water from atmospheric air. The tautomeric polymorphism of N_7-G and N_9-G purine rings provides a new insight in nucleic acid bases crystals.

INTRODUCTION

Guanine is the most widespread organic crystal existing in organisms to produce structural colors.[1−3] Guanine monohydrate and two anhydrous guanine phases, α and β, are three well-known crystalline phases of guanine. It was found that anhydrous guanine (AG) β phase is the main phase existing in organisms such as silvery fish and spiders,[4] while the AG α phase[5] and GM[6] in pure phase have been synthesized in vitro. The relationship of the crystal structure and the physical and chemical properties of GM had been investigated in theoretical studies[7−11] since the structure of GM was reported in 1971.[12] Recently, single crystalline GM microneedles were prepared by Gur et al. by varying the pH values of the solution for the first time.[6]

Tautomerization related issues are fundamentally important and challenging within diverse chemistry subdisciplines from conventional organic chemistry, biochemistry, to pharmaceutical chemistry to the emerging surface chemistry. Such tautomerization phenomena also extensively exist in DNA bases, which result in the presence of a variety of noncanonical tautomeric forms and may be responsible for base mismatch, mutagenesis, and genetic damage.[13,14] Tautomeric polymorphs—pairs of tautomers crystallizing in different crystal structures with no other or identical components—are very rare, which is also called desmotropy.[15,16] A 2011 systematic survey of the Cambridge Structural Database (CSD) showed that as of that date there were only 16 cases of this phenomenon.[15,17] Tautomeric polymorphs are seldom possible in solids.[18] Guanine is an essential component of DNA and RNA. As one of the four canonical bases, guanine has the largest number of tautomers, and the two most stable ones are the canonical N_7-protonated tautomer (N_7-G) form and the N_9-protonated tautomer (N_9-G) form.[19] Both of the α and β phase AG crystals are composed of N_7-G, while GM is composed of N_9-G. However, a tautomeric polymorph of anhydrous guanine composed of a N_7-G purine ring has never been reported in the literature as far as we know.

Guanosine derivatives are ideal building blocks for the fabrication of complex architectures with highly controlled rigidity and have been applied as ion channels and molecular optoelectronics.[20−25] Lipophilic guanosine derivatives can form either H-bonded ribbons, quartet-based columnar structures through different self-assembly pathways.[20,26,27] In the presence of cations, guanosine derivatives can form macrocyclic G-quartets, which may further self-assemble into G_9-M^+ octamers.[21,28] Doluca and co-workers reviewed the strategies aimed at altering the properties of guanine-rich oligonucleotides (GROs) using chemical tools, which provide novel strategies to manipulate DNA/RNA assemblies by using GROs.[29] Wu and co-workers prepared bioinspired crystalline organic frameworks using G-quadruplexes as intrinsic electron donors linking planar aromatic electron acceptors, which exhibited excellent structural stability and electrical conductivity as cathode materials in a Li-ion battery.[30]

Herein, we realized the synthesis of dehydrated-GM, which is the first reported tautomeric polymorph of AG. The

Received: April 22, 2018
Revised: September 27, 2018
Published: October 16, 2018

DOI: 10.1021/acs.cgd.8b00606
Cryst. Growth Des. 2018, 18, 6497−6503

Scheme 1. Two Major Keto-Amino Tautomers of Guanine, (a) the N_7-G Form and (b) the N_9-G Form Are in Aqueous Solution. (c) The Guanine Ring of Reported Anhydrous Guanine (AG) Consisting of N_7-G. Possible Dehydration/Hydration Process in between (d) GM and (e) Dehydrated-GM through Heating and Cooling. The crystal structures of AG and GM were drawn according to literature.[6]

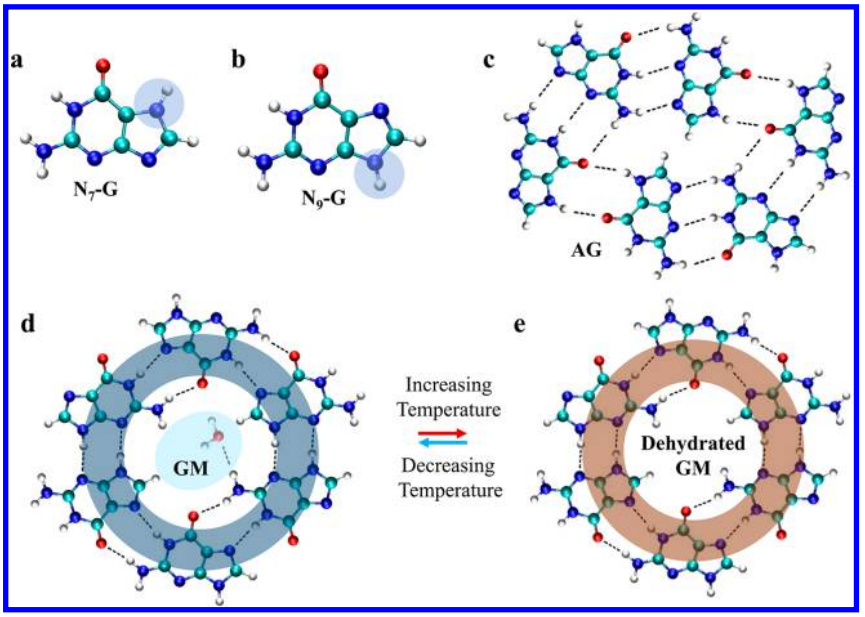

dehydrated-GM is monoclinic crystal composed of N_9-G, tautomeric polymorph of AG (N_7-G). The dehydrated-GM has long-term stability at room temperature and robust stability after repetitive water harvest from atmospheric air. Reversible and efficient dehydration/hydration transformation between GM and dehydrated-GM can proceed in large scale, probably due to their similar crystal structures and the elaborate water channels composed of six N_9-G molecules.

EXPERIMENTAL SECTION

Materials. Industry guanine ($C_5H_5N_5O$) was bought from Alfa Aesar. Sodium hydroxide (NaOH) was bought from Xilong Scientific. Sulfuric acid (H_2SO_4) was bought from Beijing Chemical Works. Cetyltrimethylammonium bromide (CTAB) was bought from Sinopharm Chemical Reagent.

Synthesis. *Synthesis of GM Nanofibers.* 3.78 g of industry guanine particles (0.025 mol) and 4.00 g of sodium hydroxide (0.10 mol) were dissolved in water (250 mL), and NaOH solution with guanine (0.1 M guanine in 0.4 M NaOH solution) was obtained, which was termed as G-Na solution in this work. 0.7 mL of sulfuric acid (0.2 M) solution was quickly added into a mixed solution of 0.5 mL of G-Na solution and 9 mL of water (pH 12−13). The final acidic solution (pH ≈ 2.5) became slightly cloudy in several minutes and was stirred at room temperature overnight. White particles of guanine were precipitated in the vessel.

Synthesis of GM Nanorods. 0.5 mL of 0.2 M H_2SO_4 solution was quickly added into a mixed solution of 0.5 mL of above G-Na solution and 9 mL of neutral PBS solution with surfactant cetyltrimethylammonium bromide (CTAB). The concentration of CTAB in final solution was 2.7 mM. The final solution (pH ≈ 7−8) was stirred at room temperature for 2 h. White precipitates can be observed in the solution after several minutes.

The synthesis of GM nanofibers in large scale: 100 mL of the above G-Na solution was slowly added into a mixed solution of 2 L of deionized water and 200 mL of 0.2 M H_2SO_4 solution. The final solution was stirred overnight. All the obtained guanine precipitates were separated by centrifugation or filtration and washed with double distilled water twice.

Characterizations of Guanine Samples. The obtained GM samples were characterized by transmission electron microscopy (TEM, FEI Tecnai T20, 200 kV), powder X-ray diffraction (PXRD, Rigaku Dmax-2000, Cu Kα; Philips X'Pert Pro, Cu Kα), scanning electron microscopy (SEM, Hitachi FE-S4800, 5 and 10 kV), and thermogravimetric analysis (TGA, TA Q600, nitrogen or air, 10 K/min).

Dehydration/Hydration Transformation. The dehydration/hydration transformation between GM and dehydrated-GM in a few milligrams was investigated by using TGA (TA Q600, nitrogen or air, 10 K/min), varying temperature powder X-ray diffraction (VT-PXRD, Philips X'Pert Pro, Cu Kα), and varying temperature Fourier transform IR spectroscopy (VT-FTIR, Nicolet Magna-IR 750 with a heating stage). The reversible transformation between GM and dehydrated-GM were tested by TGA, VT-XRD, and VT-FTIR for more than 10 cycles. The crystal lattice parameters of dehydrated-GM at 150 °C and GM at room temperature were calculated by Topas with profile-fitting (Pawley Method) according to the PXRD patterns. The dehydration process of GM in large scale (1.5 g) at room temperature with different humidities was investigated, while the temperature was increased step by step from 40 to 120 °C in the oven. The obtained dehydrated-GM was then hydrated while the temperature of the oven was decreased to 80 °C. The oven was kept at a certain temperature for 30 min to let the dehydration/hydration transformation proceed, and an analytical balance was applied to record the weight change every 10 min. The weight variation of the same amount of GM was reexamined reversibly at different room humidities more than three times. A dynamic vapor sorption analyzer (TA Q5000SA) was applied to study the water absorption rate of dehydrated-GM under different humidities. GM was transferred to dehydrated-GM in a TG furnace (TA Q5000SA) at 80 °C with humidity 0%. The temperature in the TG furnace was then reduced to 40 °C. The hydration rates for dehydrated-GM at 40 °C was tracked by increasing the humidity from 0% to 70% step by step. The samples were maintained for 1 h at each humidity.

RESULTS

Characterizations of a Novel Anhydrous Guanine Phase, Dehydrated-GM. N_7-G and N_9-G are two major keto-amino tautomers of guanine, as shown in Scheme 1.

Guanine is insoluble in water but can be easily dissolved in acidic or alkali aqueous solution.[31,32] In this work, guanine was

DOI: 10.1021/acs.cgd.8b00606
Cryst. Growth Des. 2018, 18, 6497−6503

first dissolved in 0.4 M NaOH basic aqueous solution at pH ≈ 12, termed as G-Na solution. Then, 0.2 M H_2SO_4 solution was quickly added into the above G-Na solution, and an acidic solution was formed (at pH ≈ 2.5). The samples obtained under acidic conditions were single crystalline GM nanofibers according to the SEM and TEM images, SAED pattern (Figure 1a,b), and powder X-ray diffraction (PXRD) pattern (Figure 1d). Diffraction spots with lattice distances of 3.73 Å, 9.61 Å, and 3.50 Å in the SAED pattern are attributed to (001), (110), and (111) of GM, respectively (Figure 1b). The long axis of nanofibers is parallel to the *c* axis of GM according to the SAED pattern. According to the PXRD pattern, all the diffraction peaks are (hk0) and the long axis of GM nanofibers are almost all parallel to the sample holder surface. We characterized the short GM nanorods obtained in PBS buffer solution with the presence of cationic surfactant (CTAB) (Figure 1c, d). The diffraction peak ($\bar{3}01$) appeared in the PXRD of the GM nanorods obtained in PBS buffer, while it was absent in the PXRD of GM nanofibers obtained under acidic solution (Figure 1d).

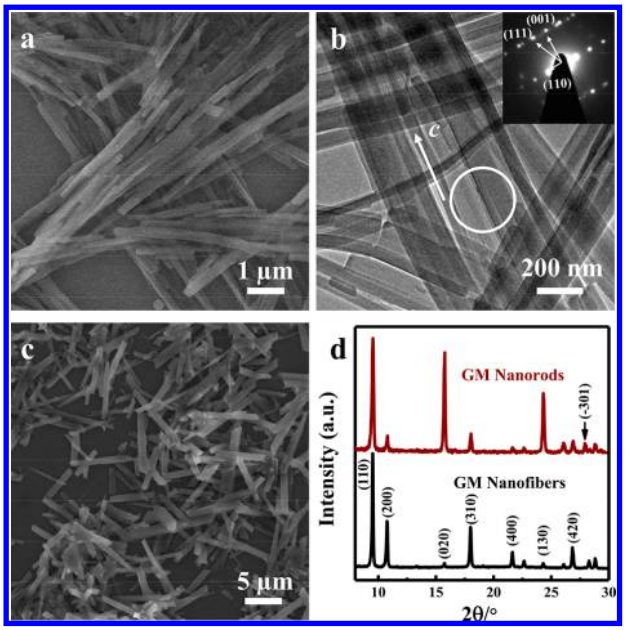

Figure 1. Characterizations of GM by using SEM, TEM, and PXRD. (a) SEM and (b) TEM images and SAED pattern (b inset) of single crystalline GM nanofibers obtained in acidic solution. (c) SEM image of GM nanorods obtained in PBS buffer with the presence of 2.7 mmol·L^{-1} CTAB. (d) Powder X-ray diffraction (PXRD) of GM nanofibers and nanorods.

Thermogravimetric analysis (TGA) was applied to study the thermal stability of GM (Figure 2). There is an endothermic peak at around 111 °C according to the DSC plot. The sample lost about 8.6 wt % when the temperature increased from room temperature (RT) to ~113 °C from the TG analysis, indicating the loss of the crystalline water at ~111 °C. There was no obvious weight loss from 113 to 350 °C according to the TGA plot. The theoretical weight percent of crystalline water in GM is 10.7%. Therefore, we propose that our synthetic GM crystals had slightly less crystalline water than the theoretical content. Furthermore, the incorporation of impurity (e.g., sulfate) in the reaction system can also contribute to such a discrepancy. There was an exothermic peak at around 232 °C, and no weight variation appears at this temperature, which indicates a phase change happens at this temperature.

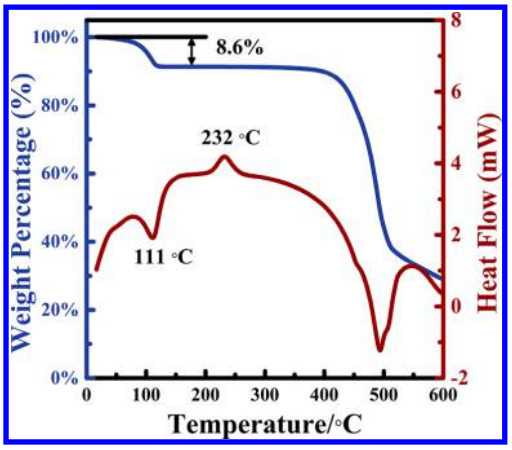

Figure 2. Characterizations of GM nanofibers by using DSC-TGA.

Varying temperature PXRD (VT-PXRD) and varying temperature Fourier transform infrared spectroscopy (VT-FTIR) were applied to follow the crystal phase variation of the GM crystals with the increase of temperature from room temperature to 250 °C (Figure 3). The VT-PXRD and VT-FTIR of typical GM nanofibers obtained under acidic solution were proceeded from RT to 250 °C. All the diffraction peaks shift to higher 2θ from those of GM, while the temperature was increased to 150 °C (Figure 3a, b). When the temperature further decreased to RT, the guanine products transformed to GM according to the PXRD pattern and IR spectrum. The PXRD patterns for the hydrated guanine samples after a few hydration/dehydration cycles are similar to that of GM, indicating that the dehydrated-GM and GM are stable under the hydration/dehydration processes and this is a reversible process (Figure 3a). The guanine products obtained at 120 and 150 °C have similar PXRD patterns (Figure 3a, b). We conclude that the guanine samples obtained at 120 and 150 °C have a novel crystal phase of anhydrous guanine with similar crystal structure of GM, termed dehydrated-GM. GM transformed to dehydrated-GM at around 111 °C according to the TGA-DSC results in Figure 2. The dehydrated-GM is stable in between 113 and 232 °C according to the DSC-TGA data (Figure 2) and VT-PXRD patterns (Figure 3c). The VT-PXRD diffraction patterns indicate that dehydrated-GM further transformed to AG when the temperature varied from 220 to 250 °C (Figure 3c), which is consistent with the exothermic peak at around 232 °C in the DSC plot (Figure 2). It was reported that there was a transformation from GM to AG at a relatively low temperature (~95 °C) in Gur's paper.[6] The differences between dehydration temperature in Gur's paper and this work may be caused by different TGA analysis conditions such as the different amounts of examined materials and temperature scanning rate. However, according to our detailed studies based on DSC-TGA and VT-PXRD results, there was phase change from GM to dehydrated-GM, and then to AG while heating the GM from RT to high temperature (250 °C). When the temperature increased from 400 to 500 °C, a sharp weight loss can be observed in the TGA plot, which was attributed to the decomposition of AG (Figure 2).

The isomeric molecular structures of different guanine crystals were characterized by using VT-FTIR (Figure 4). FTIR spectra of dehydrated-GM, GM at RT and GM treated

DOI: 10.1021/acs.cgd.8b00606
Cryst. Growth Des. 2018, 18, 6497−6503

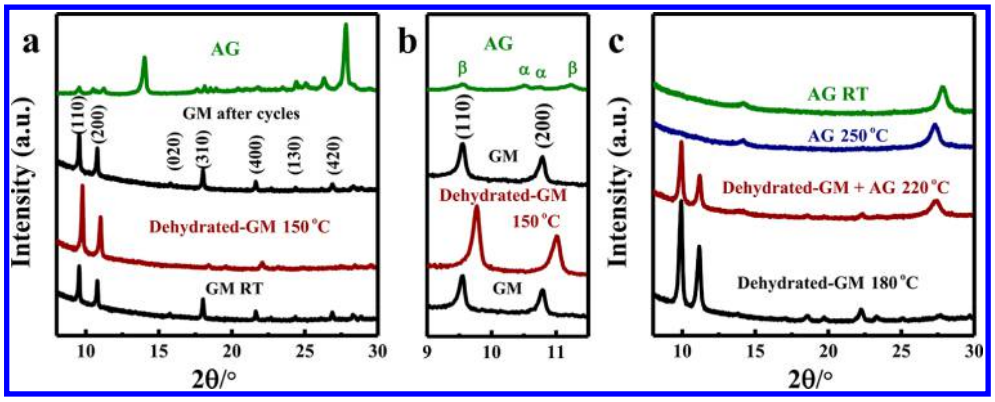

Figure 3. In-situ VT-PXRD characterization of guanine monohydrate dehydration process. Panels (a) and (b) reversible hydration/dehydration processes between dehydrated-GM (150 °C) and GM after a few dehydration hydration cycles, (c) irreversible process of dehydrated-GM to AG.

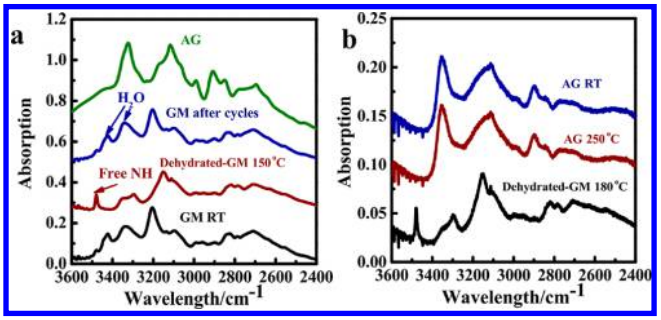

Figure 4. In-situ VT-FTIR spectroscopy of guanine monohydrate dehydration process. (a) Reversible hydration/dehydration processes between dehydrated-GM (150 °C) and GM after a few dehydration hydration cycles, (b) irreversible process of dehydrated-GM to AG.

with a few dehydration/hydration cycles are similar to that of GM reported in Gur's work[6] (Figure 4). The broad peaks at 3420 and 3200 cm^{-1} are attributed to the water stretching modes (−OH) of ν_1 and ν_3, respectively, which are absent in the IR spectra of AG and dehydrated-GM. Dehydrated-GM and GM have similar vibrations of the purine ring, N_9-G, different from AG (N_7-G), between 3600 and 2400 cm^{-1}. The IR vibration bands in between 3600 and 2400 cm^{-1} of GM, AG and dehydrated-GM (150 °C), are listed in Table 1. The

Table 1. Experimental IR Wavenumbers for Three Guanine Crystals

modes	ν_a $(NH_2)^a$/cm^{-1}	ν_s $(NH_2)^b$/cm^{-1}	ν (OH)/cm^{-1}
GM (RT)	3478 (w)[c], 3337	3137	3422, 3204
80 °C	3476 (w), 3344	3137	3425, 3202
120 °C	−, 3344	3150	3426, 3199
150 °C	3479, 3296	3151	
180 °C	3480, 3295	3154	
250 °C	3350	3113	
AG (RT)	3341	3113	

[a]ν_a: antisymmetric stretching. [b]ν_s: symmetric stretching. [c]w: weak.

NH bonds of the $-NH_2$ group of dehydrated-GM are not symmetrical (Scheme 1e), one hydrogen of $-NH_2$ forms hydrogen bond with adjacent guanine molecule (3296 cm^{-1}), and the other hydrogen of $-NH_2$ is free (3479 cm^{-1}). The free hydrogen on $-NH_2$ is unstable and has strong hydroscopicity.

Dehydrated-GM and GM have similar crystal structures according to their PXRD patterns. According to the VT-FTIR spectra, the dehydrated-GM is composed of N_9-G, which has been proposed in theory,[33] but has not been synthesized in the laboratory, as far as we know. We calculated the cell data of dehydrated-GM at 150 °C (Table 2) according to its PXRD

Table 2. Crystal Lattice Parameters of GM (RT) and Dehydrated-GM (150 °C) Were Calculated by PXRD Patterns[a]

parameters	GM (RT)	dehydrated-GM (150 °C)	variation (%)
syngony	monoclinic	monoclinic	
a (Å)	16.55	16.20	−2.1
b (Å)	11.27	10.99	−2.4
c (Å)	3.65	3.60	−1.4
β (deg)	96.6	96.1	
V (Å^3)	676.2	637.3	−6

[a]GM nanorods obtained in PBS buffer were characterized by using PXRD to calculate the crystal lattice parameters of dehydrated-GM.

pattern. Dehydrated-GM is monoclinic crystal and shrinks anisotropically along different axes in comparison to the cell data of monoclinic GM. The lattice parameter along the b axis has more shrinkage (2.4%) than those along the a axis (2.1%) and c axis (1.4%). The GM nanofibers after the dehydration/hydration process still exhibit single crystalline feature according to the TEM image and SAED pattern (Figure S1a). Small nanoparticles can be seen along the one-dimensional nanostructures while the heating temperature was 250 °C (Figure S1), while the deposition of aggregates of AG nanoparticles with needle-like morphology in this work is consistent with Gur's work.[6]

Dehydration/Hydration Process of GM. We investigated the dehydration/hydration process of GM by varying the temperature between RT (25 °C) and 150 °C, back and forth for many cycles. The weight variation and the polymorph change of the guanine samples during the dehydration/hydration process were tracked by using TGA and VT-PXRD (Figure 5a). As for the first cycle, the temperature of the TGA furnace body with dehydrated-GM was decreased from 150 °C to RT, and then increased from RT to 150 °C with a rate of 10 K/min. Almost no weight change can be detected from the TGA plot with a variation of temperature from 150 °C to RT, and vice versa, when dehydrated-GM was kept in a very dry TGA furnace body (Figure 5a, cycle 1). Dehydrated-GM regained about 5 wt % due to the partial hydration to GM, while it was exposed to the atmospheric air for 30 s at RT (25 °C, 70% RH) (cycle 2). Dehydrated-GM transformed to GM

DOI: 10.1021/acs.cgd.8b00606
Cryst. Growth Des. 2018, 18, 6497−6503

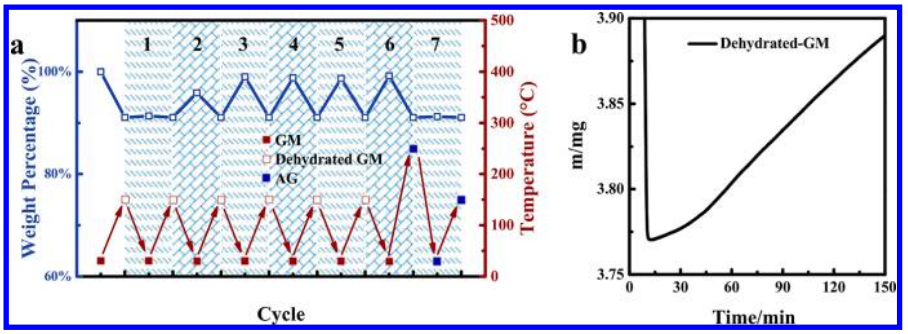

Figure 5. Characterizations on the hydration/dehyration process of GM in small scale. (a) Reversible water absorption ability of dehydrated-GM from atomospheric air. (b) Dehydrated-GM formed at 150 °C from GM was kept in a very dry furnace body (below 20% humidity), and the weight of the guanine was recorded with time.

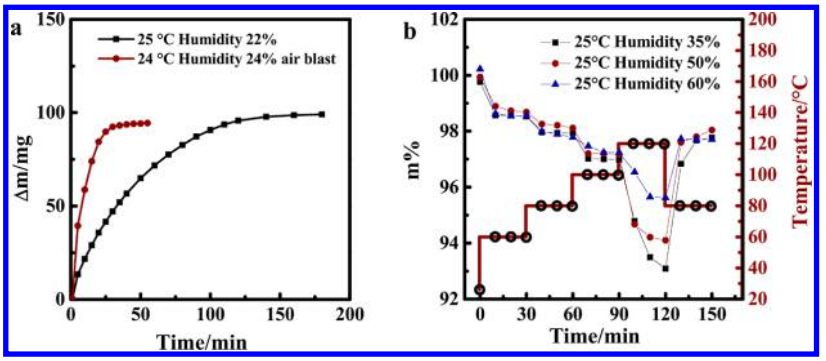

Figure 6. Characterizations on the hydration/dehyration process of GM in large scale. (a) About 1.5 g of GM treated at 120 °C was then exposed to air at RT, and the increasing weight of dehydrated-GM was recorded with time under standing and air blowing conditions. (b) The dehydration/hydration process of 1.5 g of GM was tested at different humidities and different temperatures, while the O locations were the measurement points for recording the sample weight.

and the sample regained about 8 wt % when dehydrated-GM was exposed to the air at RT for 2 min (cycle 3, first part). GM further lost crystalline water and transformed to dehydrated-GM after reheating the system to 150 °C (cycle 3, second part). We repeated the dehydration/hydration process three times, and similar weight variation results were obtained (cycle 3−5). Dehydrated-GM regained water and transformed to GM in the first part for the sixth cycle. However, GM further transformed to AG after reheating the system to 250 °C (cycle 6, the second part). The phase transformation from GM to AG when the temperature increased to 250 °C was confirmed from the VT-PXRD patterns (Figure 3c). No obvious weight change can be observed when the temperature varied from 250 °C to room temperature, or from RT to 150 °C (cycle 7). Different from dehydrated-GM, AG could not transform to GM when it was exposed to the air (~25 °C, 70% RH, cycle 7, first part), probably because the crystal structure of AG is very different from GM. The dehydration/hydration process study between GM and dehydrated-GM indicates that this is a reversible process and can be repeated more than 10 times.

Obvious weight gaining (8 wt %) can be observed in 150 min when a small amount of dehydrated-GM (~4 mg) was kept in the DSC-TGA furnace body with dry N_2 flow under low humidity (less than 20% RH) at room temperature. The hydration rate of dehydrated-GM was nearly linear in 150 min under the above condition (Figure 5b). Dehydrated-GM can "acquire" 8 wt % water from the atmospheric air in half an hour under low humidity (below 20% RH). The hydration process of dehydrated-GM at 40 °C was studied in the TGA furnace body while increasing the humidity step by step from 10% to 70% (Figure S2). Dehydrated-GM exhibits a very good ability to acquire water even when the humidity is as low as 20−30%. More importantly, dehydrated-GM can adsorb one molar water and transform to GM at relatively low humidity and low temperature (40 °C and 40% humidity) using dynamic vapor sorption (DVS) analyzer (Figure S2). The hydration property of dehydrated-GM in large scale (gram-scale) was further investigated (Figure 6). First, after a dehydration process at 120 °C for 30 min, GM transformed to dehydrated-GM. The weight of increment water on dehydrated-GM was tracked with time at RT and low humidity (24−25 °C, 20−24% humidity) (Figure 6a). The hydration rate was fast, and about 95% of dehydrated-GM in gram-scale transformed to GM in 30 min at room temperature when there was air blowing (Figure 6a). It can be seen that the hydration rate of dehydrated-GM was obviously faster when air blowing was applied than the standing case. Dehydrated-GM has a fast hydration feature both in small and large scales.

We proceeded the dehydration/hydration process of a large amount of GM (~1.5 g) while increasing the temperature step by step from room temperature (25 °C) to 120 °C and then decreasing the temperature to 80 °C under controlled humidity. The weight variations of guanine samples were studied with time while changing the temperature and humidity (Figure 6b). Under different room humidities (35% and 50%), the weight loss varied from 2 to 4 wt % when the temperature increased from 100 to 120 °C, much more than that at low temperature window (60 to 100 °C). One possible reason is that most of the crystalline water was removed while increasing the temperature from 100 to 120 °C. The

DOI: 10.1021/acs.cgd.8b00606
Cryst. Growth Des. 2018, 18, 6497−6503

dehydration process of GM took about 30 min at 120 °C. In contrast, the hydration process from dehydrated-GM to GM can be finished in about 10 to 20 min while decreasing the temperature from 120 to 80 °C, much faster than the dehydration process. The weight loss at low humidity (35%) was 5 wt %, more than two times higher than that at high humidity (65%) when the temperature was increased from 100 to 120 °C, which indicates that the water partial pressure is essential to the dehydration/hydration process.

DISCUSSION

Tautomeric polymorph systems provide an exceptional opportunity for studying tautomeric forms separately, which is of key importance for canonical bases.[18] As one of the most popular organic crystals exist in many organisms,[2] AG composed of a N_7-G purine ring is very different from the guanine molecule (N_9-G) existing in DNA/RNA. In this work, we realized the formation of a novel polymorph of anhydrous guanine, dehydrated-GM (N_9-G), the first reported tautomeric polymorph of AG (N_7-G). As far as we know, this is also the first time the tautomeric polymorph of canonical bases has been reported, which may be potentially applied for investigations for base mismatch, mutagenesis, and genetic damage. The discovery of dehydrated-GM (N_9-G) provides a new insight in nucleic acid bases crystals and may have potential applications,[34,35] e.g., wide band gap semiconductors.[35]

Atmospheric water is a resource equivalent to ∼10% of all fresh water in lakes on Earth, and thus water harvest from atmospheric air may be a good choice to solve severe water scarcity.[36] There are mainly two kinds of mechanisms for atmospheric water adsorption: (1) chemical reactions, e.g., $CaCl_2$; (2) physical adsorption on the internal surface, porous materials like zeolites, metal organic frameworks (MOFs).[37] The reversible hydration/dehydration process of MOFs has been applied as a water collecting system.[38] The dehydrated-GM can adsorb about 8 wt % water from a relatively dry atmospheric environment (20% RH) within 30 min, which is very fast in comparison to other water harvest materials. The zigzag channel in the GM crystal structure might contribute to the fast movement of water molecule and the fast hydration/dehydration rate under low humidity. The dehydration/hydration process between GM and dehydrated-GM can be repeated more than 10 times, and the same phase variation phenomenon can be observed in our experiments, which indicates the high stability of dehydrated-GM in between RT and 150 °C. Further experiments indicate that the dehydrated-GM can be stable at high temperature (150 °C) for overnight. One possible reason for the high stability of dehydrated-GM is that the crystal structure of dehydrated-GM does not change much from that of GM, and only a slight shrinking (less than 2.4%) along different crystalline axes happens when GM transforms to dehydrated-GM. Only one water molecule can have hydrogen bonding with guanine molecules in the inner channel of guanine crystal, in which six guanine molecules form a six-membered ring plane through hydrogen bonding. The pores of dehydrated-GM are very appropriate for water adsorption. Thus, the dehydrated-GM has high selectivity for water adsorption. Due to the advantages such as the high stability, high selectivity, the high water harvest rate at low humidity (20%) or relatively low temperature (40 °C), and the reversal hydration/dehydration feature, dehydrated-GM can be applied as a good potential water harvest material in the future.

CONCLUSION

The dehydration process of GM was investigated in detail and phase variation from GM to dehydrated-GM, and then to AG was observed for the first time. The dehydrated-GM is a novel crystalline phase (N_9-G), the first reported tautomeric polymorph of AG (N_7-G), which may have potential application in biological chemistry and biomedical engineering. This is also the first time the tautomeric polymorph of canonical bases has been reported. The dehydrated-GM has very high stability at high temperature (150 °C) for overnight, and the dehydration/hydration process between GM and dehydrated-GM can be repeated more than 10 times. The dehydrated-GM has very good water harvest ability (8 wt %) with a fast rate (in 30 min) even at relatively low room humidity (below 20%) and low temperature (40 °C). Therefore, dehydrated-GM may have potential application as a water harvest material in a dry environment.

ASSOCIATED CONTENT

Supporting Information

The Supporting Information is available free of charge on the ACS Publications website at DOI: 10.1021/acs.cgd.8b00606.

Figure S1. Characterizations on the guanine samples after being treated at high temperature. Figure S2. Dynamic vapor sorption analysis of dehydrated-GM in TG furnace (PDF)

AUTHOR INFORMATION

Corresponding Authors

*(Y.M.) E-mail: yurong.ma@bit.edu.cn.
*(L.Q.) E-mail: liminqi@pku.edu.cn.

ORCID

Yurong Ma: 0000-0002-2432-5614
Limin Qi: 0000-0003-4959-6928

Notes

The authors declare no competing financial interest.

ACKNOWLEDGMENTS

Financial support from the National Key R&D Program of China (2018YFC1105101), National Natural Science Foundation of China (Grant No. 21622301), and Beijing Institute of Technology Research Fund Program for Young Scholars is gratefully acknowledged.

REFERENCES

(1) Pascual, E.; Addadi, L.; Andres, M.; Sivera, F. Mechanisms of crystal formation in gout-a structural approach. *Nat. Rev. Rheumatol.* **2015**, *11*, 725.

(2) Gur, D.; Palmer, B. A.; Weiner, S.; Addadi, L. Light manipulation by guanine crystals in organisms: Biogenic scatterers, mirrors, multilayer reflectors and photonic crystals. *Adv. Funct. Mater.* **2017**, *27*, 1603514.

(3) Palmer, B. A.; Taylor, G. J.; Brumfeld, V.; Gur, D.; Shemesh, M.; Elad, N.; Osherov, A.; Oron, D.; Weiner, S.; Addadi, L. The image-forming mirror in the eye of the scallop. *Science* **2017**, *358*, 1172.

(4) Hirsch, A.; Gur, D.; Polishchuk, I.; Levy, D.; Pokroy, B.; Cruz-Cabeza, A. J.; Addadi, L.; Kronik, L.; Leiserowitz, L. "Guanigma": The revised structure of biogenic anhydrous guanine. *Chem. Mater.* **2015**, *27*, 8289.

(5) Guille, K.; Clegg, W. Anhydrous guanine: a synchrotron study. *Acta Crystallogr., Sect. C: Cryst. Struct. Commun.* **2006**, *62*, O515.

(6) Gur, D.; Pierantoni, M.; Dov, N. E.; Hirsh, A.; Feldman, Y.; Weiner, S.; Addadi, L. Guanine crystallization in aqueous solutions

DOI: 10.1021/acs.cgd.8b00606
Cryst. Growth Des. 2018, 18, 6497−6503

enables control over crystal size and polymorphism. *Cryst. Growth Des.* **2016**, *16*, 4975.
(7) Gorb, L.; Leszczynski, J. Intramolecular proton transfer in mono- and dihydrated tautomers of guanine: An ab initio post Hartree-Fock study. *J. Am. Chem. Soc.* **1998**, *120*, 5024.
(8) Monajjemi, M.; Honarparvar, B.; Nasseri, S. M.; Khaleghian, M. NQR and NMR study of hydrogen bonding interactions in anhydrous and monohydrated guanine cluster model: A computational study. *J. Struct. Chem.* **2009**, *50*, 67.
(9) Parac, M.; Doerr, M.; Marian, C. M.; Thiel, W. QM/MM calculation of solvent effects on absorption spectra of guanine. *J. Comput. Chem.* **2010**, *31*, 90.
(10) Shukla, M. K.; Leszczynski, J. Guanine in water solution: Comprehensive study of hydration cage versus continuum solvation model. *Int. J. Quantum Chem.* **2010**, *110*, 3027.
(11) Yu, L. J.; Pang, R.; Tao, S.; Yang, H. T.; Wu, D. Y.; Tian, Z. Q. Solvent effect and hydrogen bond interaction on tautomerism, vibrational frequencies, and raman spectra of guanine: A density functional theoretical study. *J. Phys. Chem. A* **2013**, *117*, 4286.
(12) Thewalt, U.; Bugg, C. E.; Marsh, R. E. Crystal structure of guanine monohydrate. *Acta Crystallogr., Sect. B: Struct. Crystallogr. Cryst. Chem.* **1971**, *27*, 2358.
(13) Goodman, M. F. DNA models - Mutations caught in the act. *Nature* **1995**, *378*, 237.
(14) Wang, W. N.; Hellinga, H. W.; Beese, L. S. Structural evidence for the rare tautomer hypothesis of spontaneous mutagenesis. *Proc. Natl. Acad. Sci. U. S. A.* **2011**, *108*, 17644.
(15) Cruz-Cabeza, A. J.; Groom, C. R. Identification, classification and relative stability of tautomers in the cambridge structural database. *CrystEngComm* **2011**, *13*, 93.
(16) Elguero, J. Polymorphism and desmotropy in heterocyclic crystal structures. *Cryst. Growth Des.* **2011**, *11*, 4731.
(17) Marshall, M. G.; Lopez-Diaz, V.; Hudson, B. S. Single-crystal x-ray diffraction structure of the stable enol tautomer polymorph of barbituric acid at 224 and 95 k. *Angew. Chem., Int. Ed.* **2016**, *55*, 1309.
(18) Rubcic, M.; Uzarevic, K.; Halasz, I.; Bregovic, N.; Malis, M.; Dilovic, I.; Kokan, Z.; Stein, R. S.; Dinnebier, R. E.; Tomisic, V. Desmotropy, polymorphism, and solid-state proton transfer: Four solid forms of an aromatic *o*-hydroxy schiff base. *Chem. - Eur. J.* **2012**, *18*, 5620.
(19) Zhang, C.; Xie, L.; Wang, L.; Kong, H.; Tan, Q.; Xu, W. Atomic-scale insight into tautomeric recognition, separation, and interconversion of guanine molecular networks on Au(111). *J. Am. Chem. Soc.* **2015**, *137*, 11795.
(20) Spada, G. P.; Lena, S.; Masiero, S.; Pieraccini, S.; Surin, M.; Samorì, P. Guanosine-based hydrogen-bonded scaffolds: Controlling the assembly of oligothiophenes. *Adv. Mater.* **2008**, *20*, 2433.
(21) Davis, J. T.; Spada, G. P. Supramolecular architectures generated by self-assembly of guanosine derivatives. *Chem. Soc. Rev.* **2007**, *36*, 296.
(22) Arnal-Herault, C.; Pasc, A.; Michau, M.; Cot, D.; Petit, E.; Barboiu, M. Functional G-quartet macroscopic membrane films. *Angew. Chem., Int. Ed.* **2007**, *46*, 8409.
(23) Sivakova, S.; Rowan, S. J. Nucleobases as supramolecular motifs. *Chem. Soc. Rev.* **2005**, *34*, 9.
(24) Bhattacharyya, T.; Kumar, Y. P.; Dash, J. Supramolecular Hydrogel Inspired from DNA Structures Mimics Peroxidase Activity. *ACS Biomater. Sci. Eng.* **2017**, *3*, 2358.
(25) Bhattacharyya, T.; Saha, P.; Dash, J. Guanosine-Derived Supramolecular Hydrogels: Recent Developments and Future Opportunities. *ACS Omega* **2018**, *3*, 2230.
(26) Giorgi, T.; Grepioni, F.; Manet, I.; Mariani, P.; Masiero, S.; Mezzina, E.; Pieraccini, S.; Saturni, L.; Spada, G. P.; Gottarelli, G. Gel-like lyomesophases formed in organic solvents by self-assembled guanine ribbons. *Chem. - Eur. J.* **2002**, *8*, 2143.
(27) El Garah, M.; Perone, R. C.; Bonilla, A. S.; Haar, S.; Campitiello, M.; Gutierrez, R.; Cuniberti, G.; Masiero, S.; Ciesielski, A.; Samori, P. Guanosine-based hydrogen-bonded 2D scaffolds: metal-free formation of G-quartet and G-ribbon architectures at the solid/liquid interface. *Chem. Commun.* **2015**, *51*, 11677.
(28) Sutyak, K. B.; Zavalij, P. Y.; Robinson, M. L.; Davis, J. T. Controlling molecularity and stability of hydrogen bonded G-quadruplexes by modulating the structure's periphery. *Chem. Commun.* **2016**, *52*, 11112.
(29) Doluca, O.; Withers, J. M.; Filichev, V. V. Molecular engineering of guanine-rich sequences: Z-DNA, DNA triplexes, and G-quadruplexes. *Chem. Rev.* **2013**, *113*, 3044.
(30) Wu, Y. L.; Horwitz, N. E.; Chen, K. S.; Gomez-Gualdron, D. A.; Luu, N. S.; Ma, L.; Wang, T. C.; Hersam, M. C.; Hupp, J. T.; Farha, O. K.; Snurr, R. Q.; Wasielewski, M. R. G-quadruplex organic frameworks. *Nat. Chem.* **2016**, *9*, 466.
(31) Devoe, H.; Wasik, S. P. Aqueous solubilities and enthalpies of solution of adenine and guanine. *J. Solution Chem.* **1984**, *13*, 51.
(32) Oaki, Y.; Kaneko, S.; Imai, H. Morphology and orientation control of guanine crystals: A biogenic architecture and its structure mimetics. *J. Mater. Chem.* **2012**, *22*, 22686.
(33) Ortmann, F.; Hannewald, K.; Bechstedt, F. Charge transport in guanine-based materials. *J. Phys. Chem. B* **2009**, *113*, 7367.
(34) Gomez, E. F.; Venkatraman, V.; Grote, J. G.; Steckl, A. J. Exploring the potential of nucleic acid bases in organic light emitting diodes. *Adv. Mater.* **2015**, *27*, 7552.
(35) Albuquerque, E. L.; Fulco, U. L.; Freire, V. N.; Caetano, E. W. S.; Lyra, M. L.; de Moura, F. A. B. F. DNA-based nanobiostructured devices: The role of quasiperiodicity and correlation effects. *Phys. Rep.* **2014**, *535*, 139.
(36) Klemm, O.; Schemenauer, R. S.; Lummerich, A.; Cereceda, P.; Marzol, V.; Corell, D.; van Heerden, J.; Reinhard, D.; Gherezghiher, T.; Olivier, J.; Osses, P.; Sarsour, J.; Frost, E.; Estrela, M. J.; Valiente, J. A.; Fessehaye, G. M. Fog as a fresh-water resource: Overview and perspectives. *Ambio* **2012**, *41*, 221.
(37) Canivet, J.; Fateeva, A.; Guo, Y.; Coasne, B.; Farrusseng, D. Water adsorption in MOFs: fundamentals and applications. *Chem. Soc. Rev.* **2014**, *43*, 5594.
(38) Kim, H.; Yang, S.; Rao, S. R.; Narayanan, S.; Kapustin, E. A.; Furukawa, H.; Umans, A. S.; Yaghi, O. M.; Wang, E. N. Water harvesting from air with metal-organic frameworks powered by natural sunlight. *Science* **2017**, *356*, 430.

DOI: 10.1021/acs.cgd.8b00606
Cryst. Growth Des. 2018, 18, 6497−6503